

1 ***Exponential phase of covid19 expansion is driven by airport***

2 ***connections***

3

4 Marco Túlio Pacheco Coelho¹, João Fabricio Mota Rodrigues¹, Anderson
5 Matos Medina², Paulo Scalco³, Levi Carina Terribile⁴, Bruno Vilela², José
6 Alexandre Felizola Diniz-Filho¹ & Ricardo Dobrovolski²

7

8 *1 Departamento de Ecologia, Universidade Federal de Goiás, CP 131, 74.001-970*

9 *Goiânia, Goiás, Brazil.*

10 *2 Instituto de Biologia, Universidade Federal da Bahia, Salvador, BA, Brazil*

11 *3. Faculdade de Administração, Economia, Ciências Contábeis (FACE), Universidade*

12 *Federal de Goiás, Goiânia, Goiás, Brazil.*

13 *4. Laboratório de Macroecologia, Universidade Federal de Jataí, Jataí, GO, Brazil*

14

15

16

17

18 **Abstract**

19 The pandemic state of COVID-19 caused by the SARS CoV-2 put the world in
20 quarantine, led to hundreds of thousands of deaths and is causing an unprecedented
21 economic crisis. However, COVID-19 is spreading in different rates at different
22 countries. Here, we tested the effect of three classes of predictors, i.e., socioeconomic,
23 climatic and transport, on the rate of daily increase of COVID-19. We found that global
24 connections, represented by countries' importance in the global air transportation
25 network, is the main explanation for the growth rate of COVID-19 in different
26 countries. Climate, geographic distance and socioeconomics had a milder effect in this
27 big picture analysis. Geographic distance and climate were significant barriers in the
28 past but were surpassed by the human engine that allowed us to colonize most of our
29 planet land surface. Our results indicate that the current claims that the growth rate of
30 COVID-19 may be lower in warmer and humid tropical countries should be taken very
31 carefully, at risk to disturb well-established and effective policy of social isolation that
32 may help to avoid higher mortality rates due to the collapse of national health systems.

33

34 **Keywords:** COVID-19, SARS CoV-2, Exponential Growth Rates, Network Centrality,
35 Spatial Analysis, Socioeconomics.

36

37 **Introduction**

38 With the worldwide spread of the novel Coronavirus Disease 2019 (COVID-19),
39 caused by the SARS-CoV-2 virus, we are experiencing a declared pandemic. One of the
40 largest preoccupations about this new virus regards its notable ability to spread given
41 the absence of any effective treatment, vaccine and immunity in human populations.
42 Epidemiologists quantify the ability of infectious agents to spread by estimating the
43 basic reproduction number (R_0) statistic [1], which measures the average number of
44 people each contagious person infects. According to the World Health Organization [2],
45 the new coronavirus is transmitting at an R_0 around 1.4-2.5, which is greater than
46 seasonal influenza viruses that spread every year around the planet (median R_0 of 1.28,
47 [3]). To anticipate the timing and magnitude of public interventions and mitigate the
48 adverse consequences on public health and economy, understanding the factors
49 associated with the survival and transmission of SARS-CoV-2 is urgent.

50 Because previous experimental [4], epidemiological [5, 6] and modeling [7]
51 studies show the critical role of temperature and humidity on the survival and
52 transmission of viruses, recent studies are testing the effect of environmental variables
53 on SARS-CoV-2 [8, 9] and forecasting monthly scenarios of the spread of the new virus
54 based on climate suitability [10, *but see* 11]. Although temperature and humidity are
55 known to affect the spread and survival of other coronaviruses (i.e., SARS-CoV and
56 MERS-CoV, [12-15] using the current occurrences of SARS-CoV-2 cases to build
57 correlative climatic suitability models without taking into consideration connectivity
58 among different locations and socioeconomic conditions might be inadequate.

59 Many factors might influence the distribution of diseases at different spatial
60 scales. Climate might affect the spread of viruses given its known effect on biological
61 processes that influences many biogeographical patterns, including the distribution of

62 diseases and human behavior (e.g., [16]). Geographic distance represents the
63 geographical space where the disease spread following the distribution of hosts and has
64 also been found to explain biogeographic patterns [17-19]. Socioeconomic
65 characteristics of countries could be viewed as a proxy for the ability to identify and
66 treat infected people and for the governability necessary to make fast political decision
67 and avoid the spread of new diseases. Finally, the global transportation network might
68 surpass other factors as it can reduce the relative importance of geographic distance and
69 facilitate the spread of viruses and their vectors [20,21]. According to the International
70 Air Transport Association [22] more than 4 billion passengers traveled abroad in 2018.
71 This amount of travelers reaching most of our planet's surface represents a human niche
72 construction (i.e. global transportation network; [23]) that facilitates the global spread
73 of viruses and vectors [20,21] in the same way it facilitated the spread of invasive
74 species and domesticated animals over modern human history [23].

75 The spread of SARS-CoV-2 from central China to other locations might be
76 strongly associated with inter-country connections, which might largely surpass the
77 effect of climate suitability. Thus, at this point of the pandemic, there is still a
78 distributional disequilibrium that can generate very biased predictions based on climatic
79 correlative modeling [24]. Thus, here we used an alternative macroecological approach
80 [25], based on the geographical patterns of exponential growth rates of the disease at
81 country level, to investigate variations on the growth rates of SARS-CoV-2. We studied
82 the effect of environment, socioeconomic and global transportation controlling for
83 spatial autocorrelation that could bias model significance. By analyzing these factors,
84 we show that the exponential growth of COVID-19 at global scale is explained mainly
85 by country's importance in global transportation network (i.e., air transportation).

86

87 **Material and methods**

88 We collected the number of people infected by the COVID-19 per day from the
89 John Hopkins [26] and European Centre for Disease Prevention and Control (ECDC,
90 [27]). This data is available for 204 countries, for which 65 had more than 100 cases
91 recorded and for which time series had at least 30 days after the 100th case. We also
92 performed the analysis considering countries with more than 50 cases, but it did not
93 qualitatively change our results. Thus, we only show the results for countries with more
94 than 100 cases.

95 In our analysis, we only used the exponential portion of the time series data (i.e.
96 number of people infected per day) and excluded days after stabilization or decrease in
97 total number of cases. We empirically modelled each time series using an exponential
98 growth model for each country and calculated both the intrinsic growth rate (r) and the
99 regression coefficient of the log growth series to be used as the response variable in our
100 models. Because both were highly correlated (Person's $r = 0.97$), we used only the
101 regression coefficient to represent the growth rate of COVID-19 in our study.

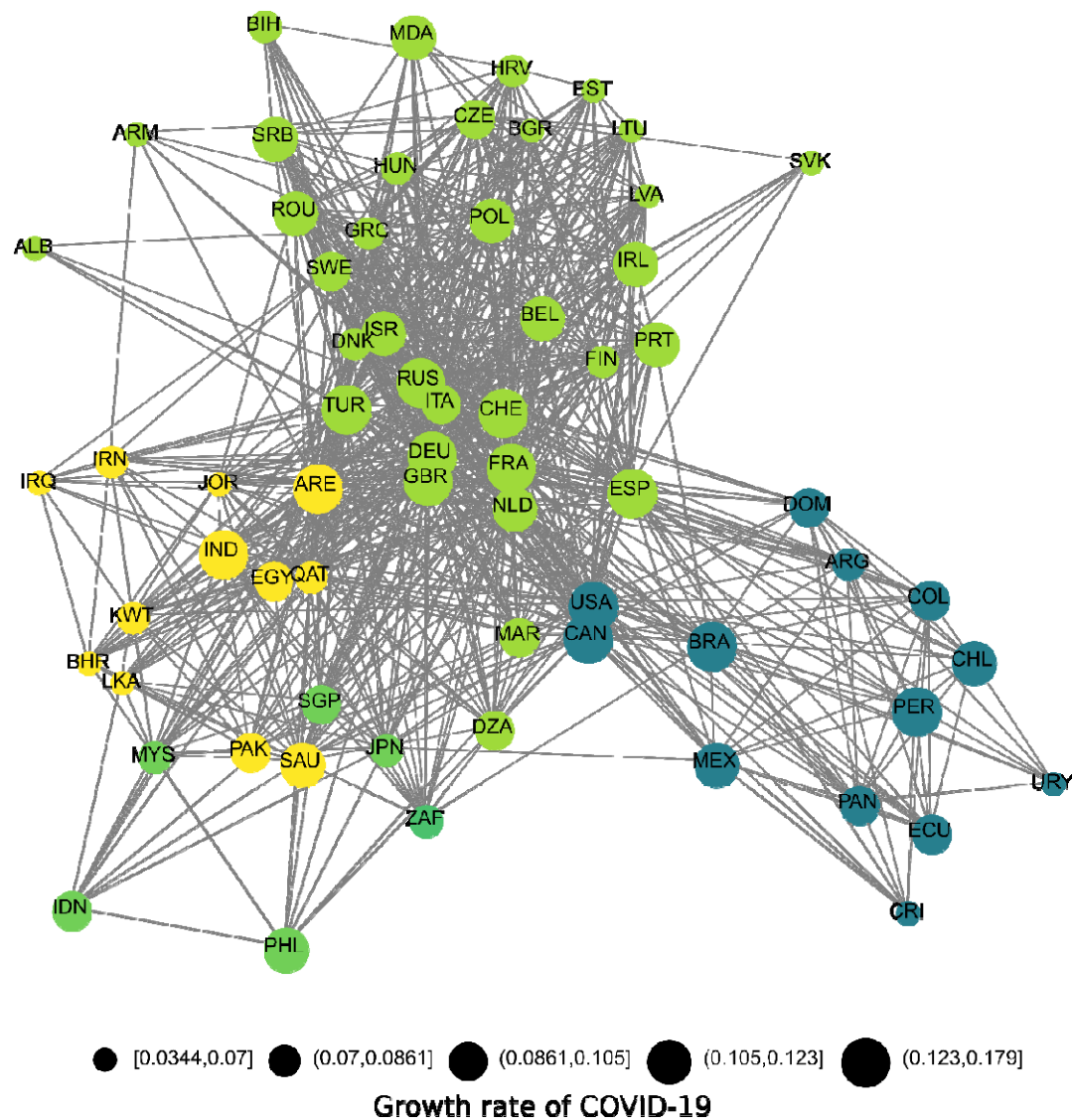
102 To investigate potential correlates of the virus growth rate, we downloaded
103 climatic and socioeconomic data of each country. We used climatic data represented by
104 monthly average minimum and maximum temperature ($^{\circ}\text{C}$) and total precipitation (mm)
105 retrieved from the WorldClim database (<https://www.worldclim.org>) [29]. We used
106 monthly available data for the most recent year available in WorldClim. We extracted
107 climatic data from the months of January, February, March, and December to represent
108 the climatic conditions of the winter season in the Northern Hemisphere and the
109 summer season in the Southern Hemisphere. From these data, we computed the mean
110 value of climatic variables across each country. Finally, minimum and maximum
111 temperatures were combined to estimate monthly mean temperature for December,

112 January, February, and March, which was used in the model along with total
113 precipitation for the same months. However, using different combinations of these
114 variables (i.e., using means of minimum or maximum temperatures, as well as
115 minimum or maximum for each month) did not qualitatively affect our results.

116 We extracted socioeconomic data for each country. Human Development Index
117 (HDI) rank, mean number of school years in 2015, gross national income (GNI) per
118 capita in 2011, population size in 2015 and average annual population growth rate
119 between 2010-2015 were used in our study and downloaded from the United Nations
120 database (<http://hdr.undp.org/en/data>). We also obtained a mean value of health
121 investment in each country by averaging the annual health investments between 2005-
122 2015 obtained from the World Health Organization database
123 (<http://apps.who.int/gho/data/node.home>). Due to the strong collinearity among some of
124 these predictors, HDI rank and mean number of school years were removed from our
125 final model.

126 Finally, we also downloaded air transportation data from the OpenFlights [30]
127 database regarding the airports of the world, which informs where each airport is
128 located including country location (7,834 airports), and whether there is a direct flight
129 connecting the airports (67,663 connections). We checked the Openflights database to
130 make the airports and connections compatible by including missing or fixing airport
131 codes and removing six unidentified airport connections resulting in a total of 7,834
132 airports and 67,657 connections. We used this information to build an air transportation
133 network that reflects the existence of a direct flight between the airports while
134 considering the direction of the flight. Thus, the airport network is a unipartite, binary,
135 and directed graph where airports are nodes and flights are links (Fig 1, Fig S1). In the
136 following step, we collapsed the airports' network into a country-level network using

137 the country information to merge all the airports located in a country in a single node
138 (e.g., United States had 613 airports that were merged in a single vertex representing the
139 country). The country-level network (Fig 1, Fig S1) is a directed weighted graph where
140 the links are the number of connections between 226 countries which is collapsed for
141 the 65 countries that had more than 100 cases and for which time series data had at least
142 30 days after the 100th case . Afterward, we measured the countries centrality in the
143 network using the Eigenvector Centrality [31], hereafter centrality, that weights the
144 importance of a country in the network considering the number of connections with
145 other countries and how well connected these countries are to other countries – indirect
146 connections. All networks analyses were generated using package *igraph* [32].
147



148

149

150 **Fig 1.** Air transportation network among 65 countries that had more than 100 cases and
151 for which time series data had at least 30 days after the 100th case. Different colours
152 represent modules of countries that are more connected to each other. Different sizes of
153 each node represent the growth rate of COVID-19 estimated for each country (See
154 results Fig 2).

155

156 We evaluated the relationship between the predictors (climatic, socioeconomic
157 and transport data) and our growth rate parameter using a standard multiple regression

158 (OLS) after taking into consideration the distribution of the original predictors as well
159 as the normality of model residuals. Moreover, OLS residuals were inspected to
160 evaluate the existence of spatial autocorrelation that could upward bias the significance
161 of predictor variables on the model using Moran's I correlograms [33]. Prior to the
162 analysis, we applied logarithmic (mean precipitation, total population size, and network
163 centrality) and square root (mean health investments) transformations to the data to
164 approximate a normal distribution.

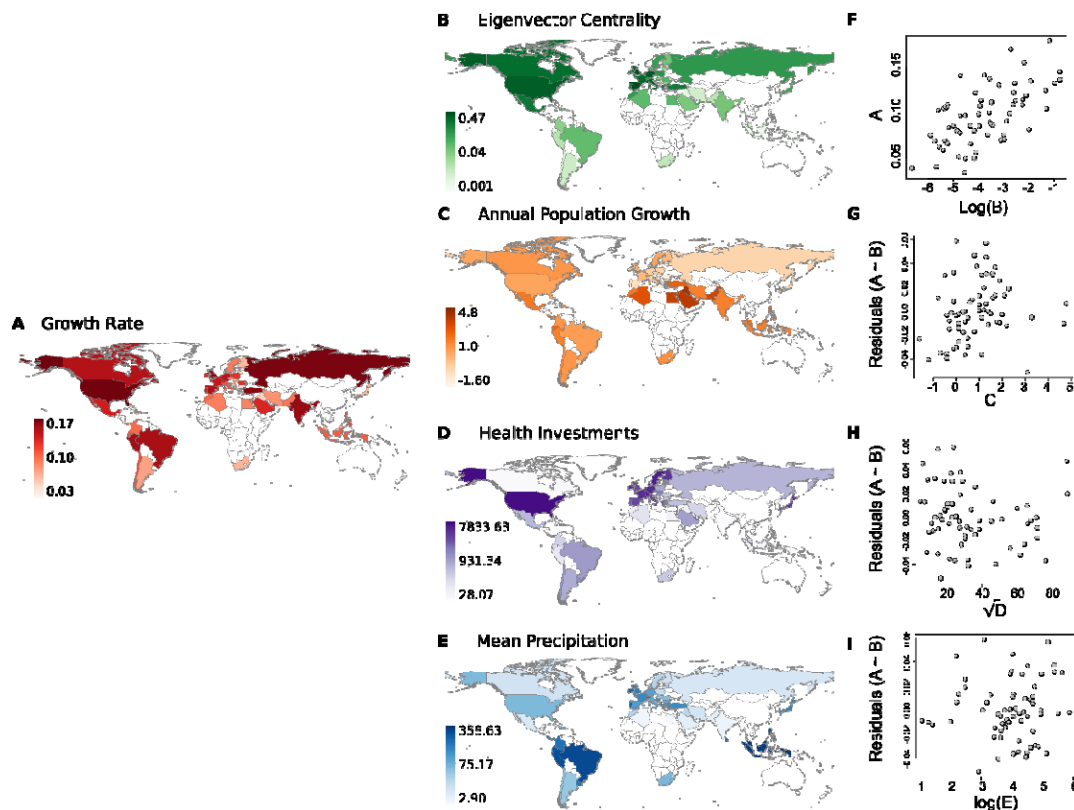
165

166 ***Results***

167 The models used to estimate COVID-19 growth rate on different countries
168 showed an average R^2 of 0.91 (SD = 0.04), varying from 0.78 to 0.99, indicating an
169 overall excellent performance on estimating growth rates. The geographical patterns in
170 the growth rates of COVID-19 cases do not show a clear trend, at least in terms of
171 latitudinal variation, that would suggest a climatic effect at macroecological scale (Fig.
172 2A).

173 We build one model including only climate and socioeconomic variables, which
174 explained *only* 14% of the variation on growth rates. This model did not have spatial
175 autocorrelation in the residuals. When we added country centrality (i.e. country
176 importance in global transportation network) as a predictor, the R^2 increased to 48.6%.
177 In this model, annual population growth and precipitation had positive and significant
178 effects (Table 1, $P = 0.036$, $P = 0.041$, Fig 2), while health investments had a negative
179 and significant effect on growth rate (Table 1, $P = 0.035$, Fig 2). Here, exponential
180 growth rates increased *strongly* in response to countries importance in the transportation
181 network which has more than two times the effect size of any significant variable (Table
182 1). However, it is also important to note that growth rates of COVID-19 weakly

183 increases with increases of annual population growth and precipitation, and decreases
184 with higher investments in health (Table 1). Statistical coefficients were not upward
185 biased by spatial autocorrelation.
186



187
188 **Fig 2.** Geographical patterns of growth rate of covid-19 in the exponential phase (A),
189 the Eigenvector Centrality that represents countries' importance in global transportation
190 network (B), Annual population growth (C), health investments (D) and mean
191 precipitation (E). The relationship between growth rate and the log transformed
192 eigenvector centrality is showed in F. G, H and I are partial plots showing the
193 relationship between the residuals of growth rates vs log transformed eigenvector
194 centrality and annual population growth, health investments and mean precipitation.
195

196 **Table 1.** Model statistics for all variables used in the study.

	Standardized				
	Estimate	Estimate	Std Error	t value	P-value
<i>Intercept</i>		0.149	0.026	3.547	< 0.001
<i>Eigenvector Centrality</i>	0.758	0.016	0.002	6.124	< 0.001
<i>Gross National Income</i>	0.16	0.000	0.000	1.491	0.141
<i>Population Size</i>	-0.096	-0.004	0.004	-0.953	0.344
<i>Annual population growth</i>	0.306	0.008	0.003	2.139	0.036
<i>Health investment</i>	-0.287	-0.0004	0.000	-2.155	0.035
<i>Mean Temperature</i>	-0.127	-0.0003	0.000	-0.908	0.367
<i>Mean Precipitation</i>	0.253	0.007	0.003	2.091	0.041

197

198

199

200 *Discussion*

201 The pandemic state of SARS CoV-2 is killing hundreds of thousands of people,
202 put the world in quarantine and is causing an unprecedented economic crisis. The rates
203 of increase of new cases of COVID-19 is faster in some countries than others. To
204 understand why growth rates are different among countries we investigate the effect of
205 climatic, socioeconomical and human transportation variables that could have important
206 roles on the exponential phase of COVID-19. At global scale, temperature, population
207 size and Gross National Income had no significant effect on the exponential phase of
208 COVID-19. However, annual population growth, health investments and precipitation
209 show significant, but weak effects on growth rates. Countries' importance in the global
210 transportation network has a key role on the severity of COVID-19 pandemic in
211 different countries as it is strongly associated with the growth rates of the disease (Fig
212 2).

213 The centrality measure is widely used to discover distinguished nodes on many
214 networks, including epidemiological networks (e.g., [34]). Our findings reinforce the
215 importance of propagule pressure on disease dissemination [35, 36]. Aerial
216 transportation is an important predictor of COVID-19 dissemination in China [37], in
217 Brazil [38], and in Mexico [39]. It is quite likely that further phases of COVID-19
218 spread, in terms of peak of infections and decrease in mortality rates, will be better
219 related to socioeconomics characteristics of each county and their political decisions
220 when secondary transmissions were identified. We can already clearly identify the
221 effects of adopting strong social isolation policies in China (see [37]) and, on the
222 opposite side of this spectrum, in European countries like Italy, Spain and England [40].
223 Our analyses call attention to the case of Brazil, a well-connected tropical country that

224 presents one of the highest increase rates of COVID-19 in the tropics in its exponential
225 phase (Fig 2A). If decision makers take into consideration yet unsupported claims that
226 growth rates of COVID-19 in its exponential phase might be lower in warmer and
227 humid countries, we might observe terrible scenarios unrolling in tropical countries,
228 especially in those with limited health care structure, such as Brazil. As our results also
229 show, those countries that invested less in health are also the ones with faster growth
230 rates of covid-19 in its exponential phase (Fig 2, Table 1).

231 When discussing and modelling the effect of climate on SARS CoV-2 it is
232 important to remember that modern human society is a complex system composed of
233 strongly connected societies that are all susceptible to rare events. It is also critical to
234 consider the negative correlations between climate and local or regional socioeconomic
235 conditions (i.e., inadequate sanitary conditions and poor nutritional conditions) that
236 could easily counteract any potential climatic effect at local scales, such as lower
237 survival rates of viruses exposed to high humidity, temperatures and high UV
238 irradiation [8, 41] Tropical regions will experience mild climate conditions in a couple
239 of months. Thus, regardless of the influence of local environmental conditions, tropical
240 countries could still expect high contagious rates. In addition, our results points to a
241 positive effect of precipitation on growth rates, which is the contrary of what has been
242 suggested by climate suitability models. Finally, climatic suitability models might be
243 ephemeral for very mathematized modelling fields of science such as epidemiology and
244 virology that developed over time very realistic models that enables the possibility of
245 learning with parameters of similar viruses (i.e. SARS) that can definitely help and
246 instruct decision makers to take actions before it is too late.

247 Here we showed that countries' importance in the global transportation network
248 has a key role on COVID-19 growth rates in its exponential phase. Our results reinforce

249 board control measures in international airports [42, 43] during exceedingly early stages
250 of pandemics to prevent secondary transmissions that could lead to undesired scenarios
251 of rapid synchronically spread of infectious diseases in different countries. The rapid
252 international spread of the severe acute respiratory syndrome (SARS) from 2002 to
253 2003 led to extensively assessing entry screening measures at international borders of
254 some countries [44, 45]. The 2019-2020 world spread of COVID-19 highlights that
255 improvements and testing of board control measures (i.e. screening associated with fast
256 testing and quarantine of infected travellers) might be a cheap solution for humanity in
257 comparison to health systems breakdowns and unprecedented global economic crises
258 that the spread of infectious disease can cause. However, it is important to note that
259 board control of potentially infected travellers and how to effectively identify them is
260 still a hotly debated topic in epidemiology and there is still no consensus on accurate
261 methodologies for its application [46].

262 We do not expect that our results using a macroecological approach at a global
263 scale would have a definitive effect on decision-making in terms of public health in any
264 particular country, province, or city. However, we expect that our analyses show that
265 current claims that growth of COVID-19 pandemics may be lower in developing
266 tropical countries should be taken very carefully, at risk to disturb well-established and
267 effective policy of social isolation that may help to avoid higher mortality rates due to
268 collapse in national health systems.

269

270 *Acknowledgments*

271 This paper was developed in the context of the human macroecology project on the
272 National Institute of Science and Technology (INCT) in Ecology, Evolution and
273 Biodiversity Conservation, supported by CNPq (grant 465610/2014-5) and FAPEG

274 (grant 201810267000023). JAFDF, RD, LCT are also supported by CNPq productivity
275 scholarships. We thank Thiago F. Rangel, André Menegotto, Robert D. Morris and
276 Marcus Cianciaruso for their constructive comments on early version of the manuscript.

277

278

279 **References**

280

- 281 1. Delamater PL, Street EJ, Leslie TF, Yang YT, Jacobsen KH. 2019
282 Complexity of the basic reproduction number (R₀). *Emerg. Infect. Dis.* **25**,
283 1–4. (doi:10.3201/eid2501.171901)
284
- 285 2. World Health Organization. 2020. Statement on the meeting of the
286 International Health Regulations (2005) *Emergency Committee regarding*
287 *the outbreak of novel coronavirus (2019-nCoV)*. Retrieved from
288 [https://www.who.int/news-room/detail/23-01-2020-statement-on-the-](https://www.who.int/news-room/detail/23-01-2020-statement-on-the-meeting-of-the-international-health-regulations-(2005)-emergency-committee-regarding-the-outbreak-of-novel-coronavirus-(2019-ncov))
289 [meeting-of-the-international-health-regulations-\(2005\)-emergency-](https://www.who.int/news-room/detail/23-01-2020-statement-on-the-meeting-of-the-international-health-regulations-(2005)-emergency-committee-regarding-the-outbreak-of-novel-coronavirus-(2019-ncov))
290 [committee-regarding-the-outbreak-of-novel-coronavirus-\(2019-ncov\)](https://www.who.int/news-room/detail/23-01-2020-statement-on-the-meeting-of-the-international-health-regulations-(2005)-emergency-committee-regarding-the-outbreak-of-novel-coronavirus-(2019-ncov))
291
- 292 3. Biggerstaff M, Cauchemez S, Reed C, Gambhir M, Finelli L. 2014 Estimates
293 of the reproduction number for seasonal, pandemic, and zoonotic influenza:
294 A systematic review of the literature. *BMC Infect. Dis.* **14**, 1–20.
295 (doi:10.1186/1471-2334-14-480)
296
- 297 4. Lowen AC, Mubareka S, Steel J, Palese P. 2007 Influenza virus transmission
298 is dependent on relative humidity and temperature. *PLoS Pathog.* **3**, 1470–
299 1476. (doi:10.1371/journal.ppat.0030151)
300
- 301 5. Shaman J, Pitzer VE, Viboud C, Grenfell BT, Lipsitch M. 2010 Absolute
302 humidity and the seasonal onset of influenza in the continental United States.
303 *PLoS Biol.* **8**. (doi:10.1371/journal.pbio.1000316)
304
- 305 6. Barreca AI, Shimshack JP. 2012 Absolute humidity, temperature, and
306 influenza mortality: 30 years of county-level evidence from the united states.
307 *Am. J. Epidemiol.* **176**, 114–122. (doi:10.1093/aje/kws259)
308
- 309 7. Zuk T, Rakowski F, Radomski JP. 2009 Probabilistic model of influenza
310 virus transmissibility at various temperature and humidity conditions.
311 *Comput. Biol. Chem.* **33**, 339–343.
312 (doi:10.1016/j.compbiolchem.2009.07.005)
313
- 314 8. Wang J, Tang K, Feng K, Lv W. 2020 High Temperature and High Humidity
315 Reduce the Transmission of COVID-19. *SSRN Electron. J.* , 1–19.
316 (doi:10.2139/ssrn.3551767)

317

- 318 9. Sajadi MM, Habibzadeh P, Vintzileos A, Shokouhi S, Miralles-Wilhelm F,
319 Amoroso A. 2020 Temperature and Latitude Analysis to Predict Potential
320 Spread and Seasonality for COVID-19. *SSRN Electron. J.* , 6–7.
321 (doi:10.2139/ssrn.3550308)
322
- 323 10. Araujo MB, Naimi B. 2020 Spread of SARS-CoV-2 Coronavirus likely to be
324 constrained by climate. *medRxiv* , 2020.03.12.20034728.
325 (doi:10.1101/2020.03.12.20034728)
326
- 327 11. Chipperfield JD. 2020 On the inadequacy of species distribution models for
328 modelling the spread of SARS-CoV-2: response to Araújo and Naimi.
329 *ecoRxiv*
330
- 331 12. Tan J, Mu L, Huang J, Yu S, Chen B, Yin J. 2005 An initial investigation of
332 the association between the SARS outbreak and weather: With the view of
333 the environmental temperature and its variation. *J. Epidemiol. Community*
334 *Health* **59**, 186–192. (doi:10.1136/jech.2004.020180)
335
- 336 13. Chan KH, Peiris JSM, Lam SY, Poon LLM, Yuen KY, Seto WH. 2011 The
337 effects of temperature and relative humidity on the viability of the SARS
338 coronavirus. *Adv. Virol.* **2011**. (doi:10.1155/2011/734690)
339
- 340 14. Doremalen NV, Bushmaker T, Munster VJ. 2013 Stability of middle east
341 respiratory syndrome coronavirus (MERS-CoV) under different
342 environmental conditions. *Eurosurveillance* **18**, 1–4. (doi:10.2807/1560-
343 7917.ES2013.18.38.20590)
344
- 345 15. Gaunt ER, Hardie A, Claas ECJ, Simmonds P, Templeton KE. 2010
346 Epidemiology and clinical presentations of the four human coronaviruses
347 229E, HKU1, NL63, and OC43 detected over 3 years using a novel
348 multiplex real-time PCR method. *J. Clin. Microbiol.* **48**, 2940–2947.
349 (doi:10.1128/JCM.00636-10)
350
- 351 16. Murray KA, Olivero J, Roche B, Tiedt S, Guégan JF. 2018 Pathogeography:
352 leveraging the biogeography of human infectious diseases for global health
353 management. *Ecography (Cop.)*. **41**, 1411–1427. (doi:10.1111/ecog.03625)
354
- 355 17. Poulin R. 2003 The decay of similarity with geographical distance in parasite
356 communities of vertebrate hosts. *J. Biogeogr.* **30**, 1609–1615.
357 (doi:10.1046/j.1365-2699.2003.00949.x)
358
- 359 18. Nekola JC, White PS. 1999 The distance decay of similarity in biogeography
360 and ecology. *J. Biogeogr.* **26**, 867–878. (doi:10.1046/j.1365-
361 2699.1999.00305.x)
362
- 363 19. Warren DL, Cardillo M, Rosauer DF, Bolnick DI. 2014 Mistaking
364 geography for biology: inferring processes from species distributions. *Trends*
365 *Ecol. {&} Evol.* **29**, 572–580. (doi:10.1016/j.tree.2014.08.003)

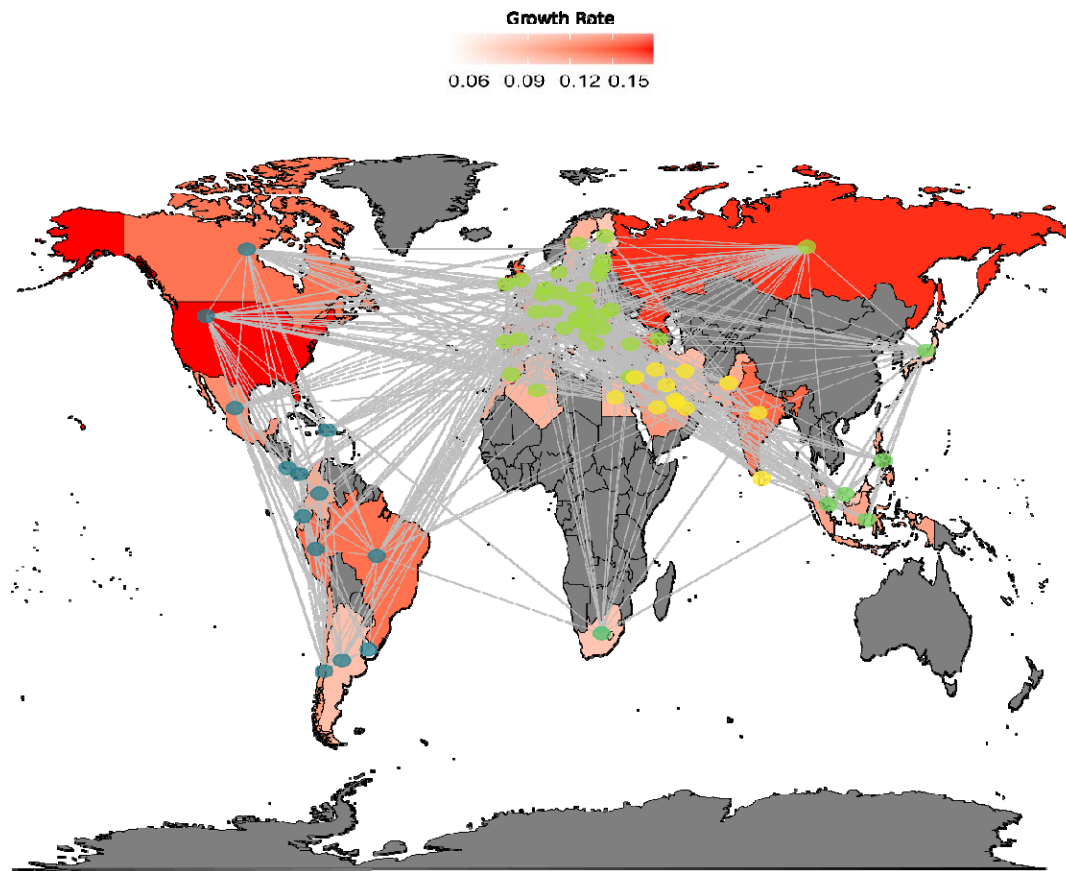
- 366
367
368
369
370
371
372
373
374
375
376
377
378
379
380
381
382
383
384
385
386
387
388
389
390
391
392
393
394
395
396
397
398
399
400
401
402
403
404
405
406
407
408
409
410
411
412
20. Brockmann D, Helbing D. 2013 The hidden geometry of complex, network-driven contagion phenomena. *Science (80)*. **342**, 1337–1342. (doi:10.1126/science.1245200)
 21. Pybus OG, Tatem AJ, Lemey P. 2015 Virus evolution and transmission in an ever more connected world. *Proc. R. Soc. B Biol. Sci.* **282**, 1–10. (doi:10.1098/rspb.2014.2878)
 22. International Air Transport Association. 2019. Annual Review(<https://www.iata.org/contentassets/c81222d96c9a4e0bb4ff6ced0126f0bb/iata-annual-review-2019.pdf>)
 23. Boivin NL, Zeder MA, Fuller DQ, Crowther A, Larson G, Erlandson JM, Denham T, Petraglia MD. 2016 Ecological consequences of human niche construction: Examining long-term anthropogenic shaping of global species distributions. *Proc. Natl. Acad. Sci. U. S. A.* **113**, 6388–6396. (doi:10.1073/pnas.1525200113)
 24. De Marco P, Diniz-Filho JAF, Bini LM. 2008 Spatial analysis improves species distribution modelling during range expansion. *Biol. Lett.* **4**, 577–580. (doi:10.1098/rsbl.2008.0210)
 25. Burnside WR, Brown JH, Burger O, Hamilton MJ, Moses M, Bettencourt LMA. 2012 Human macroecology: linking pattern and process in big-picture human ecology. *Biol. Rev.* **87**, 194–208. (doi:10.1111/j.1469-185X.2011.00192.x)
 26. Dong E, Du H, Gardner L. 2020 An interactive web-based dashboard to track COVID-19 in real time. *Lancet Infect. Dis.* **20**, 533–534. (doi:10.1016/S1473-3099(20)30120-1)
 27. European Centre for Disease Prevention and Control (ECDC). COVID-19 - Situation update – worldwide. Stockholm: ECDC; 1 Apr 2020. Available from: <https://www.ecdc.europa.eu/en/geographical-distribution-2019-ncov-cases>
 28. Harris I, Jones PD, Osborn TJ, Lister DH. 2014 Updated high-resolution grids of monthly climatic observations - the CRU TS3.10 Dataset. *Int. J. Climatol.* **34**, 623–642. (doi:10.1002/joc.3711)
 29. Fick SE, Hijmans RJ. 2017 WorldClim 2: new 1-km spatial resolution climate surfaces for global land areas. *Int. J. Climatol.* **37**, 4302–4315. (doi:10.1002/joc.5086)
 30. Openflights.org database. 2014. <http://openflights.org/data.html>. Accessed 20 March 2020

- 413 31. Bonacich P. 1987 Power and Centrality: A Family of Measures. *Am. J.*
414 *Sociol.* **92**, 1170–1182. (doi:10.1086/228631)
- 415
416 32. Csardi G, Nepusz T. 2006. The igraph software package for complex
417 network research. *InterJournal, Complex Systems*, 1695. <http://igraph.org>.
418
- 419 33. Legendre P, Legendre L. Numerical Ecology. Elsevier Science.
420
- 421 34. Madotto A, Liu J. 2016 Super-Spreader Identification Using Meta-
422 Centrality. *Sci. Rep.* **6**, 1–10. (doi:10.1038/srep38994)
423
- 424 35. Tian H *et al.* 2017 Increasing airline travel may facilitate co-circulation of
425 multiple dengue virus serotypes in Asia. *PLoS Negl. Trop. Dis.* **11**, 1–15.
426 (doi:10.1371/journal.pntd.0005694)
427
- 428 36. Chinazzi M *et al.* 2020 The effect of travel restrictions on the spread of the
429 2019 novel coronavirus (COVID-19) outbreak. *Science* **9757**, 1–12.
430 (doi:10.1126/science.aba9757)
431
- 432 37. Kraemer MUG *et al.* 2020 The effect of human mobility and control
433 measures on the COVID-19 epidemic in China. *Science* **497**, 493–497.
434 (doi:10.1126/science.abb4218)
435
- 436 38. Ribeiro SP *et al.* 2020 Severe airport sanitarian control could slow down the
437 spreading of COVID-19 pandemics in Brazil. *medRxiv* ,
438 2020.03.26.20044370. (doi:10.1101/2020.03.26.20044370)
439
- 440 39. Dattilo W, Silva AC, Guevara R, McGregor-Fors I, Pontes S. 2020 COVID-
441 19 most vulnerable Mexican cities lack the public health infrastructure to
442 face the pandemic: a new temporally-explicit model. *medRxiv* , 1–13.
443 (doi:10.1101/2020.04.10.20061192)
444
- 445 40. Enserink, M & Kupferschmidt, K. (2020). Mathematics of life and death:
446 How disease models shape national shutdowns and other pandemic policies.
447 *Science* ([https://www.sciencemag.org/news/2020/03/mathematics-life-and-](https://www.sciencemag.org/news/2020/03/mathematics-life-and-death-how-disease-models-shape-national-shutdowns-and-other#)
448 [death-how-disease-models-shape-national-shutdowns-and-other#](https://www.sciencemag.org/news/2020/03/mathematics-life-and-death-how-disease-models-shape-national-shutdowns-and-other#))
449
- 450 41. Duan S-M *et al.* 2003 Stability of SARS coronavirus in human specimens
451 and environment and its sensitivity to heating and UV irradiation. *Biomed.*
452 *Environ. Sci.* **16**, 246–255.
453
- 454 42. Bitar D. , Goubar A. DJC. 2009 International travels and fever screening
455 during epidemics: a literature review on the effectiveness and potential use
456 of non-contact infrared thermometers. *Euro Surveill* **14**, pii=19115.
457
- 458 43. Nishiura H, Kamiya K. 2011 Fever screening during the influenza (H1N1-
459 2009) pandemic at Narita International Airport, Japan. *BMC Infect. Dis.* **11**,
460 1–11. (doi:10.1186/1471-2334-11-111)
461

- 462 44. Bell DM *et al.* 2004 Public health interventions and SARS spread, 2003.
463 *Emerg. Infect. Dis.* **10**, 1900–1906. (doi:10.3201/eid1011.040729)
464
- 465 45. John St. RK, King A, De Jong D, Bodie-Collins M, Squires SG, Tam TWS.
466 2005 Border screening for SARS. *Emerg. Infect. Dis.* **11**, 6–10.
467 (doi:10.3201/eid1101.040835)
468
- 469 46. Sun G., Matsui T., Kirimoto T., Yao Y., Abe S. .2017. Applications of
470 Infrared Thermography for Noncontact and Noninvasive Mass Screening of
471 Febrile International Travelers at Airport Quarantine Stations. In: Ng E.,
472 Etehadtavakol M. (eds) Application of Infrared to Biomedical Sciences.
473 Series in BioEngineering. Springer, Singapore
474
- 475

476

477



478

479 **Fig S1.** Spatial pattern of the air transportation network among 65 countries that had
480 more than 100 cases and for which time series data had at least 30 days after the
481 100th case. Red colours in different countries represent different growth rates of
482 COVID-19 in each country. Different colours in the nodes represent modules of
483 countries that are more connected to each other